Biocatalysis

Molecular Dynamics Simulations Guide Chimeragenesis and Engineered Control of Chemoselectivity in Diketopiperazine Dimerases

Vikram V. Shende, Natalia R. Harris, Jacob N. Sanders, Sean A. Newmister, Yogan Khatri, Mohammad Movassaghi, Kendall N. Houk,* and David H. Sherman*

Abstract: In the biosynthesis of the tryptophan-linked dimeric diketopiperazines (DKPs), cytochromes P450 selectively couple DKP monomers to generate a variety of intricate and isomeric frameworks. To determine the molecular basis for selectivity of these biocatalysts we obtained a high-resolution crystal structure of selective Csp^2–N bond forming dimerase, AspB. Overlay of the AspB structure onto C–C and C–N bond forming homolog NzeB revealed no significant structural variance to explain their divergent chemoselectivities. Molecular dynamics (MD) simulations identified a region of NzeB with increased conformational flexibility relative to AspB, and interchange of this region along with a single active site mutation led to a variant that catalyzes exclusive C–N bond formation. MD simulations also suggest that intermolecular C–C or C–N bond formation results from a change in mechanism, supported experimentally through use of a substrate mimic.

$\boldsymbol{D}$iketopiperazine (DKP) natural products (NPs) have been isolated from all kingdoms of life, with over 1300 identified to date.[1] The structures of DKP-containing NPs are highly diverse, and many possess densely functionalized scaffolds as a result of extensive and selective enzymatic tailoring such as hydroxylation,[2,3] alkylation,[4] thiolation,[5]

[*] Dr. V. V. Shende, N. R. Harris, Dr. S. A. Newmister, Dr. Y. Khatri, Prof. D. H. Sherman
Life Sciences Institute, University of Michigan
Ann Arbor, MÌ 48109 (USA)
E-mail: davidhs@umich.edu

Dr. J. N. Sanders, Prof. K. N. Houk
Department of Chemistry and Biochemistry, University of California Los Angeles
Los Angeles, CA (USA)
E-mail: houk@chem.ucla.edu

Prof. M. Movassaghi
Department of Chemistry, Massachusetts Institute of Technology
Cambridge, MA 02139 (USA)

nitration,[6] nitrone oxidation,[7] desaturation,[8] dealkylation,[9] prenyltransfer and terpene cyclization,[10] oxidative cyclization,[11] coupling to nucleotides,[12] spirocyclization,[13,14] Diel–Alder cycloaddition,[15] and dimerization.[16] The tryptophan-linked dimeric DKP NPs are of particular interest as dimers are isolated both as single compounds and mixtures of constitutional isomers. This suggests that the selectivity of dimerization (and therefore site of C–H functionalization) is under enzymatic control.[17,18] Prior to the isolation of the (+)-naseseazine B (**1**), all tryptophan-linked DKP dimers had been isolated from fungi. Identification of new bacterial DKP dimers has expanded significantly in the past decade (Figure 1), including annotation of the associated biosynthetic gene clusters (BGCs) for (+)-naseseazine constitutional isomers (−)-naseseazine C (**2**)[19] and C–N bond-linked metabolite (−)-aspergilazine A (**3**).[20] Recently, bacterial dimers possessing connectivities previously observed exclusively from fungi such as tetratryptomycins A–C (**4–6**),[21] have been characterized, and the decoding of their BGCs provided access to soluble surrogates for fungal cytochromes P450 (P450s), including "fungal specific" scaffolds such as the $C_{7'}$-C_3-linked (+)-pestalazine A (**7**),[17,22] and $C_{7'}$-C_2-linked luchunazine D (**8**).[23

Previously, we characterized the versatile DKP dimerase, NzeB, that catalyzes dimerization of brevianamide F (**9**) into carbon-carbon (C_6–C_3) linked dimer, (+)-naseseazine B (**1**),[24,25] C_5–C_3 linked (−)-naseseazine C (**2**)[26] as well as the carbon-nitrogen (C–N) linked dimer (−)-aspergilazine A (**3**).[27] Structural characterization of NzeB revealed two monomers of **9** bound in discrete pockets in the active site, and through mutagenesis of these residues we were able to abrogate formation of C–N linked dimers as well as perturb the product distribution of C–C linked dimers. However, neither homologous substitution nor alanine scanning mutagenesis of the NzeB active site generated a variant able to catalyze exclusive formation of the C_6–N_1 linked dimer, **3**. Despite extensive screening, we were unable to capture NzeB-substrate complexes that displayed a binding mode with substrates preorganized to form the C_6–N_1 dimerization axis found in **3**. Concomitant to our efforts, Yu et al. identified dimerase AspB (97% amino acid identity to NzeB),[20] which exclusively catalyzes dimerization of **9** into **3**. Based on this new functional information, we hypothesized that the molecular basis for selective intermolecular
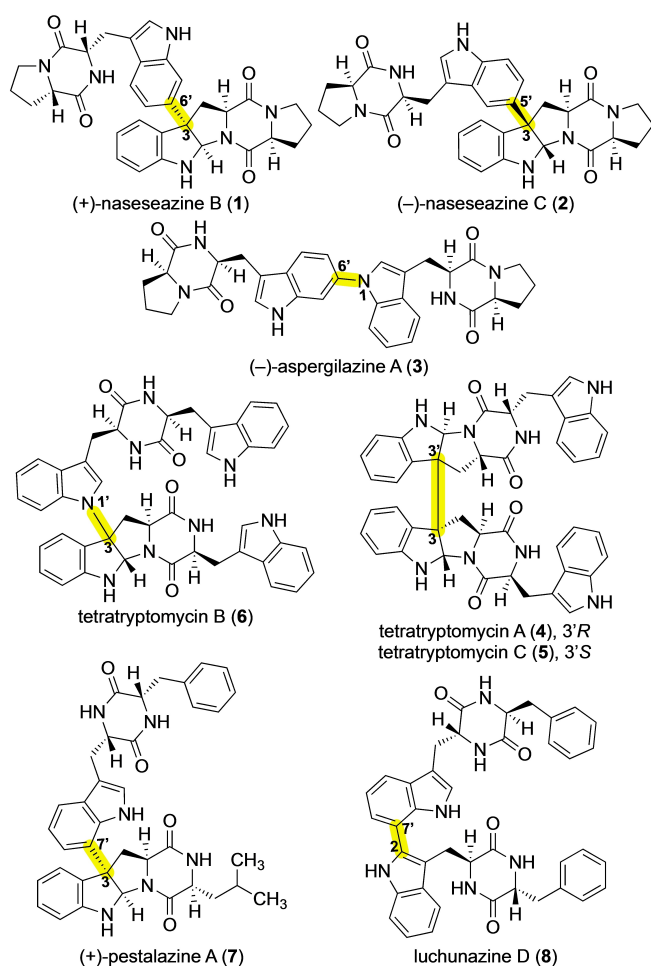
Figure 1. Tryptophan-linked DKP homodimers representative of known dimerization connectivities found exclusively in bacteria (1–2), those common to bacteria and fungi (3–6), and exclusive to fungal DKP dimers (7–8).
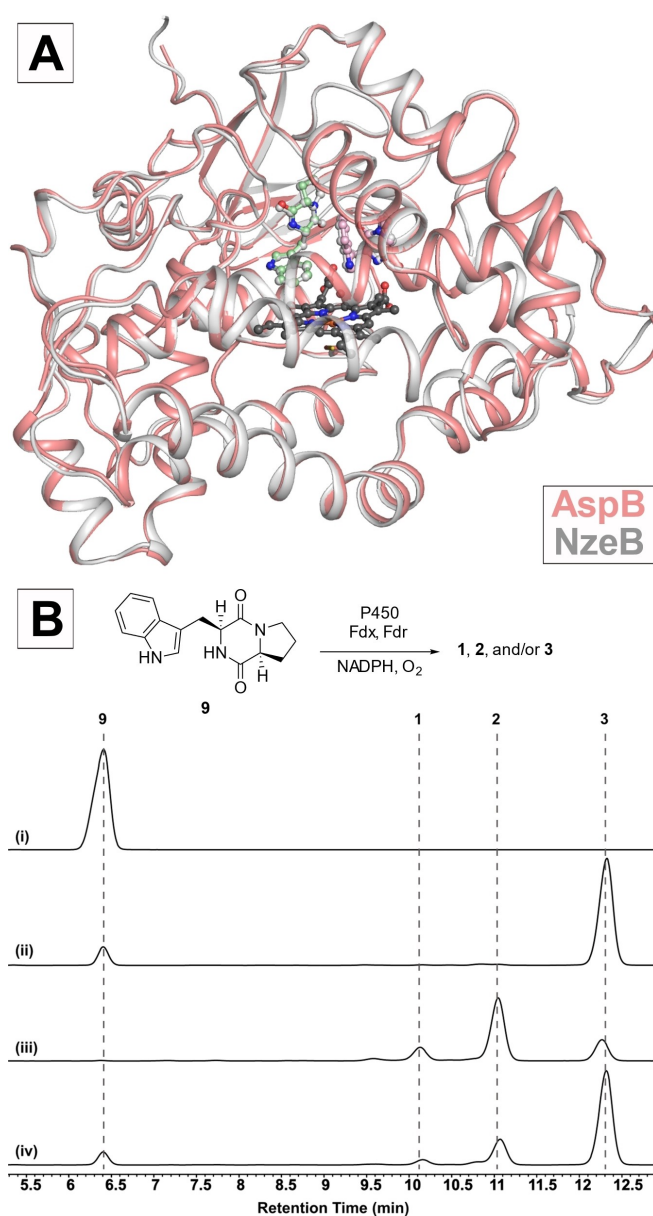

Figure 2. A) Crystal structure of AspB (salmon) with substrates bound in cyclization site (pink) and dimerization site (mint green), heme (dark grey) and overlayed with NzeB (light grey) and its bound substrates (light grey). B) HPLC traces of (i) 9 synthetic standard, (ii) reaction of 9 with AspB, (iii) reaction of 9 with NzeB, and (iv) reaction of 9 with NzeB$_{Q68I}$. Fdx and Fdr are ferredoxin and ferredoxin reductase, respectively (*S. oleracea*).

C_6–N_1 bond formation would become evident through structural characterization of P450 AspB.

To this end, we solved its x-ray crystal structure in complex with two units of **9** bound in the active site (PDB: 7S3J).[28] Despite their orthogonal chemoselectivity, the overall structure of AspB is completely superimposable with NzeB (root mean square deviation, RMSD = 0.39 Å) and substrates in each enzyme are bound in coincident positions and conformations (Figure 2A). Given this conservation of protein structure and substrate organization, we reasoned the single amino acid variation between active sites of AspB and NzeB (AspB = Ile68, NzeB = Gln68) may account for the observed switch in chemoselectivity between these dimerases (Figure 2B). To evaluate the role of this active site variation in dimerization selectivity, we generated variant NzeB$_{Q68I}$. Dimerization reactions with NzeB$_{Q68I}$ resulted in increased production of **3**, however full reconstitution of AspB selectivity was not observed (Figure 2B). To identify potential substrate-enzyme interactions unique to AspB that may facilitate selective intermolecular C_6–N_1 bond formation, we performed extensive alanine-scanning

mutagenesis of the AspB active site and evaluated selectivity of these variants (Supporting Information, Supplementary Figure S3), however the resulting variants did not perturb the distribution of C–C or C–N linked dimers, implicating residues distal to the active site as drivers of dimerization chemoselectivity.

As the divergent selectivities of the NzeB/AspB dyad could not be attributed to major variations in either sequence or structure, this motivated us to employ molecular dynamics (MD) simulations to identify the structural

Angew. Chem. **2023**, *135*, e202210254 (2 of 6)

© 2023 The Authors. Angewandte Chemie published by Wiley-VCH GmbH

elements that influence dimerase selectivity.[29–31] Thus, we performed 1.2 microsecond simulations of each substrate-bound enzyme and to identify regions with differential conformational plasticity, we computed the RMSD for the α-carbon of each residue (averaged over all three MD simulations) compared to the crystal structure (Figure 3). Comparing the α-carbon RMSD vs. residue number for NzeB and AspB revealed a region that appeared to be considerably less flexible in AspB from residues 86–91 (Figure 3a), which also corresponds to a region with low shared sequence homology (Supporting Information, Supplementary Figure S1). Overlays of representative snapshots of the protein backbone for residues 87–90 across all three MD simulations of both enzymes revealed that the higher RMSD for this region in NzeB (and absent in AspB) is explained by the presence of an additional cluster of conformations in which residues 87–90 move away from the active site (Figure 3B). Thus, we hypothesized the decrease in flexibility between residues 87–90 in AspB may be responsible for its ability to catalyze exclusively C_6–N_1 bond formation. To functionally examine the role residues 87–90 play in the chemoselectivity of these enzymes, we generated

a chimera of AspB and NzeB, using NzeB as a template, and the dimerization selectivity of the NzeB$_{G87A-A89G-I90V}$ was evaluated in vitro (Figure 4).

Analysis of the dimerization products of NzeB$_{G87A-A89G-I90V}$ revealed a significant shift in product distribution with a clear preference for C_6–N_1 bond formation, albeit with diminished dimerization activity. Additionally, we generated and evaluated a series of chimeras from regions that MD simulations indicated were unlikely to affect selectivity, and indeed no significant change in product distribution was observed compared to wild-type NzeB (Figure 4B) and minimal perturbation of substrate turnover was observed. We then incorporated the active site variation at residue 68 into the NzeB$_{G87A-A89G-I90V}$ chimera to generate NzeB$_{Q68I-G87A-A89G-I90V}$ and dimerization reactions with this new variant
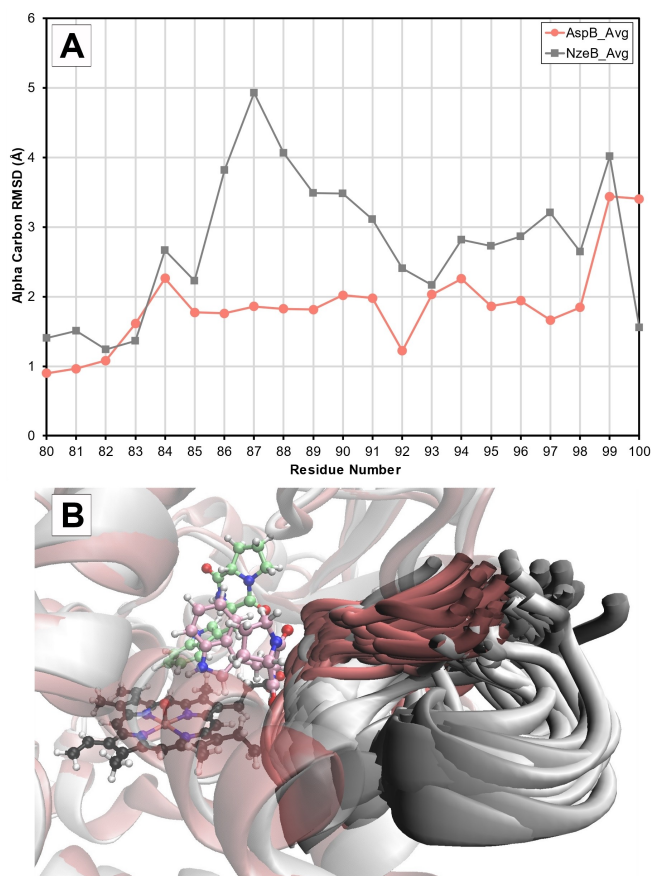

Figure 3. A) RMSD for the α-carbon of amino acids 80–100 vs. residue number for NzeB (light grey) and AspB (salmon) averaged over three 1.2 microsecond MD simulations. B) Representative snapshots of the backbone of residues 87–90 for NzeB (light grey), NzeB heme (dark grey), and AspB (salmon) taken every 24 ns over all three 1.2 microsecond MD simulations.
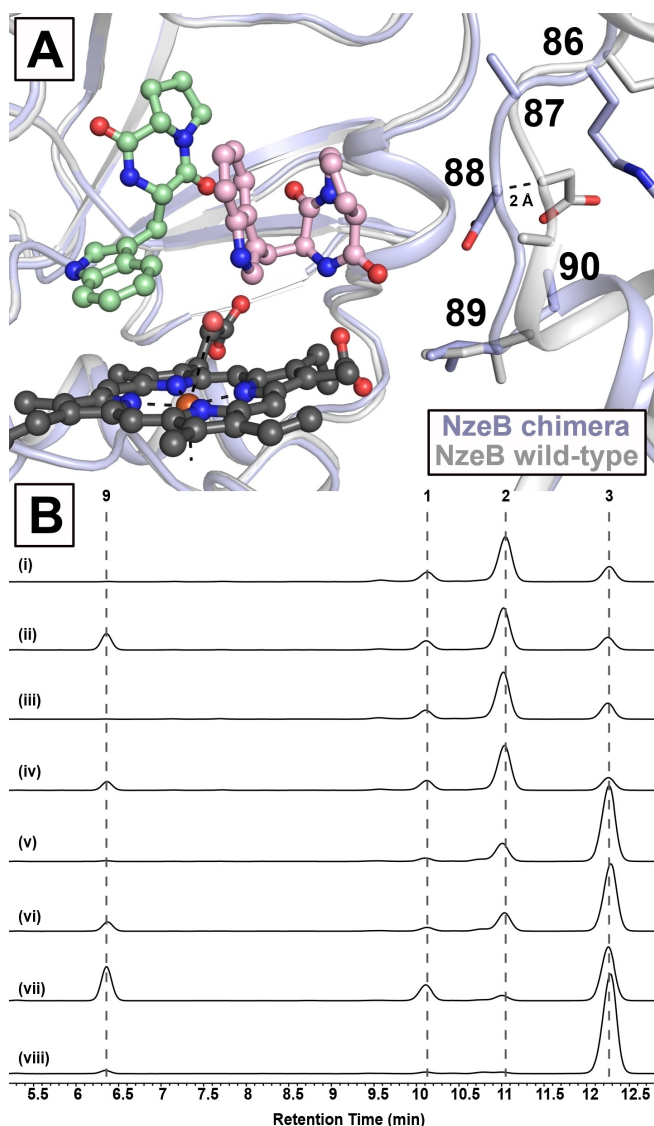

Figure 4. A) Crystal structure of NzeB$_{Q68I-G87A-A89G-I90V}$ (light blue) and NzeB wt (grey) with chimeric region labeled. B) HPLC traces from reactions of **9** with (i) wild-type NzeB, (ii) NzeB$_{P43H-V47A}$, (iii) NzeB$_{T52A-K55E}$, (iv) NzeB$_{Q222H}$, (v) NzeB$_{S60P-F62L-Q68I}$, (vi) NzeB$_{Q68I}$, (vii) NzeB$_{G87A-A89G-I90V}$, (viii) NzeB$_{Q68I-G87A-A89G-I90V}$

resulted in exclusive C_6-N_1 bond formation. Structural characterization of the NzeB$_{Q68I-G87A-A89G-I90V}$ (PDB: 7S3T)[32] revealed a clear shift in the conformation of the chimeric region compared to wild-type NzeB (Figure 4A).

Previous quantum mechanical (QM) calculations, and high-resolution structures of NzeB, informed our mechanistic hypothesis that intermolecular C–C and C–N bond formation occurs via two distinct mechanisms.[27] Our QM calculations[27] posited that dimerization cascades leading to intermolecular C–C bond formation are initiated by abstraction of the DKP N_α–H by the P450 iron-oxo species (Figure 5A, atoms and arrows colored blue). Alternatively, dimerization reactions that result in formation of C_6-N_1 bond linked dimers are initiated by indole N_1–H abstraction (Figure 5A, atom and arrows colored red). While N_1-indolyl radical and the pentacyclic C_3-carbon centered radical may interconvert, it is expected that their trapping by the dimerization partner in the active site may favor the formation of the respective products as illustrated. Comparative MD simulations of AspB and NzeB to identify the selectivity influencing regions also enabled examination of the variations in position and orientation of substrates bound in the active site of these two enzymes. MD simulations revealed that AspB maintains the indole N_1–H proximal to the iron-oxo throughout the trajectory (Figure 5B). By contrast, NzeB rapidly repositions the DKP N_α–H proximal to the P450 iron-oxo (Figure 5C), followed often by indole N_1–H and DKP N_α–H interchanging localization to the iron-oxo throughout the simulations (Supporting Information, Supplementary Figure S2), consistent with NzeB's ability to form both C–C and C–N bond linked dimers.

These MD-simulations reinforce our mechanistic hypothesis that selectivity in dimerization is dependent on remodeling of the active site and repositioning of substrates upon formation of the reactive iron-oxo species. Given the innate challenge in generation, spectroscopic observation, and definitive assignment of substrate radical intermediates, we sought to focus on experimentally validating differential binding of substrates between C–C and C–N bond forming dimerases. Thus, we synthesized three substrate mimics incapable of N–H abstraction at the N_1–H and subjected them to dimerization conditions with AspB and NzeB. While reactions with probes **S1** and **S2** failed to show differential reactivity across all P450s examined, (Supporting Information, Supplementary Figures S18–S23), reactions with substrate **10** resulted in the generation of significant quantities of a new product exclusively formed by C–C bond forming P450 NzeB, and no observable products were formed in reactions with AspB (Figure 6). High-resolution mass spectrometry revealed a product with a *m/z* of 317.0952 (M+H$^+$) (calculated=317.0954) indicative of a single oxygen insertion. Tandem MS/MS and NMR analysis enabled structural assignment of a new product **11** (Figure 6), which was further confirmed via chemical synthesis[33] and comparative analysis by HPLC (Figure 6, trace iv) and NMR. The selective formation of **11** by C–C bond forming dimerases and absence of reaction of **10** by C–N bond forming dimerases represents the first experimental evidence that chemodivergent dimerases position substrates differentially during catalysis despite completely superimposable x-ray structures.

In the current study, we determined the crystal structure of AspB, and while directed evolution campaigns have generated enzymes capable of catalyzing intra-[34] and intermolecular[35] C–H amination, AspB is the first structure of a wild-type cytochrome P450 that selectively catalyzes direct, intermolecular Csp^2–H amination. In an effort to distinguish the structural characteristics between AspB and chemodivergent homologue NzeB, we used MD simulations to compare overall conformational flexibility of these enzymes to uncover non-active site regions of the protein
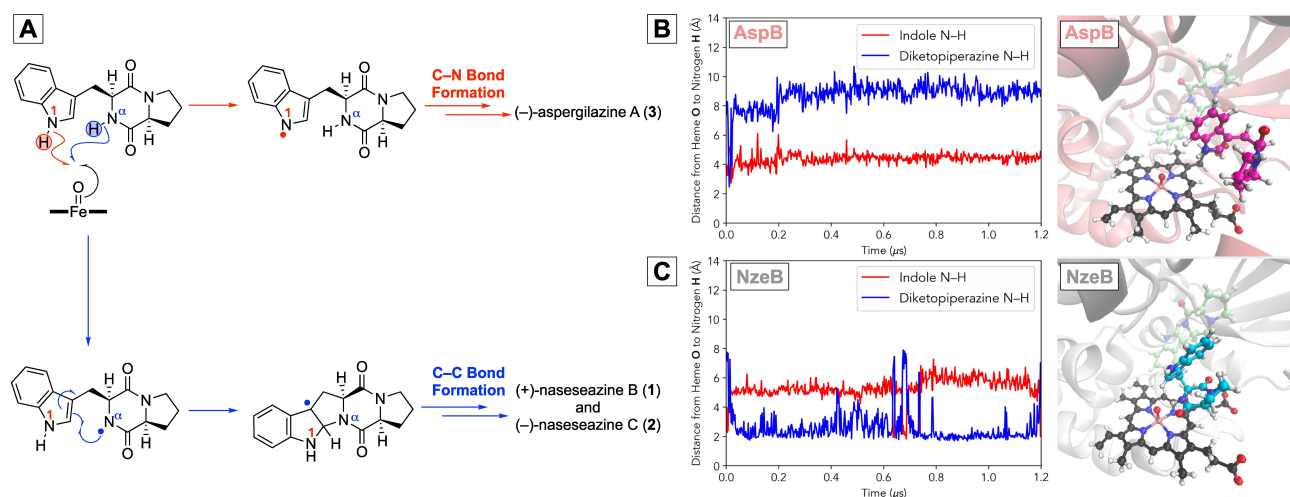

Figure 5. A) Proposed mechanistic divergence between C–C and C–N bond formation catalyzed by DKP dimerases. B) Plot showing distance from P450 iron-oxo species to indole N_1–H (red) and DKP N_α–H (blue) over the course of a 1.2 microsecond MD simulation for AspB (left) and a representative snapshot for N_1–H abstraction catalyzed by AspB. C) Corresponding distance plot and representative snapshot for the N_α–H abstraction catalyzed by NzeB.
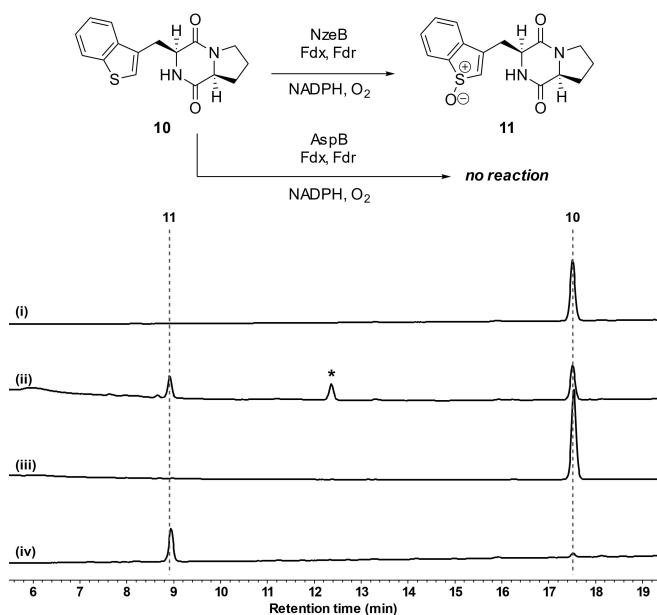
Figure 6. HPLC traces for (i) synthetic standard of **10**, (ii) reactions of **10** with C–C bond forming dimerase NzeB and (iii) C–N bond forming dimerase AspB, and (iv) synthetic standard of **11**. Asterisk indicates benzothiophene sulfone which is also exclusively generated in reactions with C–C bond forming dimerases.

that control regioselectivity in DKP dimerization. Notably, models of AspB generated via AlphaFold[36] are also nearly superimposable with our experimentally determined structures of NzeB and AspB with no reorganization of active site architecture (Supporting Information, Supplementary Figure S29). These MD simulations guided our chimeragenesis, and through exchange of a non-active site region along with a single active site residue, we generated an NzeB chimera that fully reconstituted the selective C–N bond formation of wild-type AspB. In the course of our work, another group was able to achieve a similar goal through stochastic substitution of amino acid residues in DKP dimerases.[37] However, obtaining high-resolution crystal structures of the biochemically distinct homologues NzeB and AspB offered an opportunity to develop an alternative methodology for rational protein engineering: MD-guided targeted chimeragenesis. MD simulations also allowed us to visualize substrate position and repositioning in the active site of both enzymes in the presence of the P450 iron-oxo species, which reinforced our previous mechanistic hypothesis that dimerase chemoselectivity is dictated by substrate reorganization and selective N–H abstraction. Our results with substrate mimic **10** provide the first experimental evidence for differential substrate repositioning in C–C bond forming dimerases (NzeB/NascB) generating sulfoxide **11** compared to a lack of reactivity in the C–N bond forming dimerase (AspB). While MD simulations have guided rational engineering of enzymes,[29,38,39] this work demonstrates its predictive power and utility for visualizing alternate modes of substrate binding, conformational dynamics, and selectivity when confronted with nearly complete structural homology. We expect the demonstrated ability of "MD-targeted chimeragenesis" to identify selectivity motifs and guide protein engineering will be applicable beyond cytochromes P450 and can be employed to engineer a diverse range of chimeric enzymes with improved catalytic activity and non-native selectivities.

Conflict of Interest

The authors declare no conflict of interest.

Data Availability Statement

The data that support the findings of this study are available in the supplementary material of this article. Coordinates and structures have been deposited in the Protein Data Bank (PDB) under accession codes 7S3J and 7S3T.

Keywords: Biosynthesis · Diketopiperazine · Enzyme Mechanisms · Molecular Dynamics · Natural Products

[1] A. D. Borthwick, *Chem. Rev.* **2012**, *112*, 3641–3716.

[2] J. B. Patteson, W. Cai, R. A. Johnson, K. C. Santa Maria, B. Li, *Biochemistry* **2018**, *57*, 61–65.

[3] S. Meng, W. Han, J. Zhao, X. Jian, H. Pan, G. Tang, *Angew. Chem. Int. Ed.* **2018**, *57*, 719–723; *Angew. Chem.* **2018**, *130*, 727–731.

[4] T. W. Giessen, A. M. von Tesmar, M. A. Marahiel, *Biochemistry* **2013**, *52*, 4274–4283.

[5] D. H. Scharf, N. Remme, A. Habel, P. Chankhamjon, K. Scherlach, T. Heinekamp, P. Hortschansky, A. A. Brakhage, C. Hertweck, *J. Am. Chem. Soc.* **2011**, *133*, 12322–12325.

[6] S. M. Barry, J. A. Kers, E. G. Johnson, L. Song, P. R. Aston, B. Patel, S. B. Krasnoff, B. R. Crane, D. M. Gibson, R. Loria, G. L. Challis, *Nat. Chem. Biol.* **2012**, *8*, 814–816.

[7] S. A. Newmister, C. M. Gober, S. Romminger, F. Yu, A. Tripathi, L. L. L. Parra, R. M. Williams, R. G. S. Berlinck, M. M. Joullié, D. H. Sherman, *J. Am. Chem. Soc.* **2016**, *138*, 11176–11184.

[8] S. Lautru, M. Gondry, R. Genet, J.-L. Pernodet, *Chem. Biol.* **2002**, *9*, 1355–1364

[9] Y. Tsunematsu, N. Maeda, M. Yokoyama, P. Chankhamjon, K. Watanabe, K. Scherlach, C. Hertweck, *Angew. Chem. Int. Ed.* **2018**, *57*, 14051–14054; *Angew. Chem.* **2018**, *130*, 14247–14250.

[10] T. Yao, J. Liu, Z. Liu, T. Li, H. Li, Q. Che, T. Zhu, D. Li, Q. Gu, W. Li, *Nat. Commun.* **2018**, *9*, 4091.

[11] C.-Y. Lai, I.-W. Lo, R. T. Hewage, Y.-C. Chen, C.-T. Chen, C.-F. Lee, S. Lin, M.-C. Tang, H.-C. Lin, *Angew. Chem. Int. Ed.* **2017**, *56*, 9478–9482; *Angew. Chem.* **2017**, *129*, 9606–9610.

[12] J. Liu, X. Xie, S. Li, *Angew. Chem. Int. Ed.* **2019**, *58*, 11534–11540; *Angew. Chem.* **2019**, *131*, 11658–11664.

[13] S. Li, J. M. Finefield, J. D. Sunderhaus, T. J. McAfoos, R. M. Williams, D. H. Sherman, *J. Am. Chem. Soc.* **2012**, *134*, 788–791.

[14] Y. Tsunematsu, N. Ishikawa, D. Wakana, Y. Goda, H. Noguchi, H. Moriya, K. Hotta, K. Watanabe, *Nat. Chem. Biol.* **2013**, *9*, 818–825.

[15] Y. Ye, L. Du, X. Zhang, S. A. Newmister, M. McCauley, J. V. Alegre-Requena, W. Zhang, S. Mu, A. Minami, A. E. Fraley, M. L. Adrover-Castellano, N. A. Carney, V. V. Shende, F. Qi, H. Oikawa, H. Kato, S. Tsukamoto, R. S. Paton, R. M. Williams, D. H. Sherman, S. Li, *Nat. Catal.* **2020**, *3*, 497–506.

[16] T. Saruwatari, F. Yagishita, T. Mino, H. Noguchi, K. Hotta, K. Watanabe, *ChemBioChem* **2014**, *15*, 656–659.

[17] G. Ding, L. Jiang, L. Guo, X. Chen, H. Zhang, Y. Che, *J. Nat. Prod.* **2008**, *71*, 1861–1865.

[18] X.-B. Li, Y.-L. Li, J.-C. Zhou, H.-Q. Yuan, X.-N. Wang, H.-X. Lou, *J. Asian Nat. Prod. Res.* **2015**, *17*, 182–187.

[19] W. Tian, C. Sun, M. Zheng, J. R. Harmer, M. Yu, Y. Zhang, H. Peng, D. Zhu, Z. Deng, S.-L. Chen, M. Mobli, X. Jia, X. Qu, *Nat. Commun.* **2018**, *9*, 4428.

[20] H. Yu, S.-M. Li, *Org. Lett.* **2019**, *21*, 7094–7098.

[21] J. Liu, X. Xie, S.-M. Li, *Chem. Commun.* **2020**, *56*, 11042–11045.

[22] R. P. Loach, O. S. Fenton, M. Movassaghi, *J. Am. Chem. Soc.* **2016**, *138*, 1057–1064.

[23] S. Sun, K. Ma, Q. Tao, J. Han, L. Bao, L. Liu, H. Liu, *Fitoterapia* **2018**, *125*, 266–272.

[24] R. Raju, A. M. Piggott, M. Conte, W. G. L. Aalbersberg, K. Feussner, R. J. Capon, *Org. Lett.* **2009**, *11*, 3862–3865.

[25] J. Kim, M. Movassaghi, *J. Am. Chem. Soc.* **2011**, *133*, 14940–14943.

[26] L. Buedenbender, T. Grkovic, S. Duffy, D. I. Kurtböke, V. M. Avery, A. R. Carroll, *Tetrahedron Lett.* **2016**, *57*, 5893–5895.

[27] V. V. Shende, Y. Khatri, S. A. Newmister, J. N. Sanders, P. Lindovska, F. Yu, T. J. Doyon, J. Kim, K. N. Houk, M. Movassaghi, D. H. Sherman, *J. Am. Chem. Soc.* **2020**, *142*, 17413–17424.

[28] S. A. Newmister, V. V. Shende, N. R. Harris, J. N. Sanders, Y. Khatri, M. Movassaghi, K. N. Houk, D. H. Sherman, *Protein Data Bank* **2021**, https://doi.org/10.2210/pdb7S3J/pdb.

[29] A. R. H. Narayan, G. Jiménez-Osés, P. Liu, S. Negretti, W. Zhao, M. M. Gilbert, R. O. Ramabhadran, Y.-F. Yang, L. R. Furan, Z. Li, L. M. Podust, J. Montgomery, K. N. Houk, D. H. Sherman, *Nat. Chem.* **2015**, *7*, 653–660.

[30] M. M. Gilbert, M. D. DeMars, S. Yang, J. M. Grandner, S. Wang, H. Wang, A. R. H. Narayan, D. H. Sherman, K. N. Houk, J. Montgomery, *ACS Cent. Sci.* **2017**, *3*, 1304–1310.

[31] M. D. DeMars, N. L. Samora, S. Yang, M. Garcia-Borràs, J. N. Sanders, K. N. Houk, L. M. Podust, D. H. Sherman, *J. Biol. Chem.* **2019**, *294*, 15947–15961.

[32] N. R. Harris, V. V. Shende, J. N. Sanders, S. A. Newmister, Y. Khatri, M. Movassaghi, K. N. Houk, D. H. Sherman, **2021**, *Protein Data Bank* https://doi.org/10.2210/pdb7S3T/pdb.

[33] R. Sang, A. Noble, V. K. Aggarwal, *Angew. Chem. Int. Ed.* **2021**, *60*, 25313–25317; *Angew. Chem.* **2021**, *133*, 25517–25521.

[34] J. A. McIntosh, P. S. Coelho, C. C. Farwell, Z. J. Wang, J. C. Lewis, T. R. Brown, F. H. Arnold, *Angew. Chem. Int. Ed.* **2013**, *52*, 9309–9312; *Angew. Chem.* **2013**, *125*, 9479–9482.

[35] C. K. Prier, R. K. Zhang, A. R. Buller, S. Brinkmann-Chen, F. H. Arnold, *Nat. Chem.* **2017**, *9*, 629–634.

[36] M. Mirdita, K. Schütze, Y. Moriwaki, L. Heo, S. Ovchinnikov, M. Steinegger, *bioRxiv* **2022**, https://doi.org/10.1101/2021.08.15.456425.

[37] C. Sun, Z. Luo, W. Zhang, W. Tian, H. Peng, Z. Lin, Z. Deng, B. Kobe, X. Jia, X. Qu, *Nat. Commun.* **2020**, *11*, 6251.

[38] S. Yang, M. D. DeMars, J. M. Grandner, N. M. Olson, Y. Anzai, D. H. Sherman, K. N. Houk, *J. Am. Chem. Soc.* **2020**, *142*, 17981–17988.

[39] S. C. Dodani, G. Kiss, J. K. B. Cahn, Y. Su, V. S. Pande, F. H. Arnold, *Nat. Chem.* **2016**, *8*, 419–425.